*Special Issue on*
*Nuclear Science and Technology*

ARTICLE

# Integrated magnetic separation-flotation process for uranium preconcentration from Cu–Mo sulfidic and magnetite-bearing sample

Terrence Louis A. Rosal*[1], John Rossmon M. Resuello[1], Leslie Marie B. Red[2], Lawrence Glen F. Sabaria[2], Pearlyn C. Manalo[3], Americus dC. Perez[2], Angel T. Bautista VII[2], and Djoan Kate Tungpalan[1]

[1]Department of Mining, Metallurgical and Materials Engineering, University of the Philippines Diliman, Quezon City 1101 Philippines
[2]Department of Science and Technology - Philippine Nuclear Research Institute (DOST-PNRI), Commonwealth Avenue, Diliman, Quezon City 1101 Philippines
[3]Graduate School of International Resource Sciences, Akita University, Akita City 010-8502 Japan

**ABSTRACT**

With the rising energy demand and the gradual exhaustion of conventional energy sources, the Philippines is considering nuclear energy to address this challenge. In support of this goal, this study focuses on developing an integrated magnetic separation–flotation process for uranium preconcentration from a Cu–Mo sulfidic and magnetite-bearing sample. The process aims to upgrade the uranium content for potential yellowcake production, a raw material for nuclear fuels. Preconcentration is necessary to reduce the volume of material and increase the grade of the feed to be processed in the subsequent stages, which would lower reagent consumption and potentially improve recovery. The sample contains 13.5% Fe, 0.49% Mo, and 0.57% Cu based on ICP-OES analysis, and 244 ppm U using He mode ICP-QQQ. Ore microscopy and XRD analysis identified biotite, orthoclase, chalcopyrite, molybdenite, magnetite, and chlorite as the major mineral phases, with uraninite as the principal uranium-bearing mineral. Separate flotation and magnetic separation trials were conducted to develop an integrated process flowsheet. The process consists of comminution, flotation for copper and molybdenum sulfide recovery, and magnetic separation to separate magnetite and upgrade uranium content in the non-magnetic fraction. Flotation achieved recoveries of 76% for Cu and 79% for Mo in the concentrate, which may be further processed into marketable copper and molybdenum products, while uranium recovery reached 74% in the non-magnetic fraction. Overall, the integrated preconcentration achieved a concentration ratio of 1.7 and an enrichment ratio of 1.25, increasing uranium grade to 305 ppm. These results demonstrate effective volume reduction and uranium upgrading, confirming that the process produces a suitable feed for further leaching and purification toward yellowcake production.

*Corresponding author
Email Address: **tarosal@up.edu.ph**
Date received: 30 May 2026
Dates revised: 23 July 2026
Date accepted: 30 July 2026
DOI: https://doi.org/10.54645/202619SupWKZ-49

## INTRODUCTION

Electricity consumption in the Philippines has increased rapidly over the past decade and is projected to nearly triple by 2040, placing significant pressure on the national energy system (Gulagi et al., 2021; Mondal et al., 2018). Despite this growth, the Philippines remains heavily dependent on fossil fuels, particularly coal and natural gas, which continue to dominate the electricity generation mix. This dependence has raised concerns regarding energy security, rising electricity costs, and greenhouse gas emissions.

In line with its commitments under the Paris Agreement, the Philippines has pledged to reduce greenhouse gas emissions by 75% under its Nationally Determined Contributions (NDCs), while also targeting a higher share of renewable energy in the national power mix by 2040 (Dixon et al., 2025). Consequently, the Philippine government is exploring the inclusion of nuclear power as part of its long-term energy transition strategy. Nuclear energy is considered a low-carbon and reliable baseload power source that could help strengthen energy security, stabilize electricity prices, and support national decarbonization goals (Andal et al., 2022).

**KEYWORDS**

Uranium, flotation, magnetic separation, mineral processing

A critical requirement for nuclear power generation is the availability of nuclear fuel. One of the most common raw materials used in nuclear fuel production is uranium concentrate, commonly known as yellowcake ($U_3O_8$), which is produced through the extraction and milling of uranium ore deposits. Uranium ores typically contain uranium-bearing minerals mixed with gangue and other undesired minerals that must be separated during processing. Economically recoverable uranium resources are concentrated in a limited number of countries, particularly Australia, Canada, Kazakhstan, Russia, and South Africa, with major high-grade deposits such as the McArthur River mine in Canada playing a significant role in global uranium supply (NEA, 2025).

Uranium deposits are geologically diverse and occur in several deposit types (Cuney, 2010). Because uranium mineralization varies significantly in terms of host rock, ore mineralogy, and uranium grade, uranium processing methods also differ depending on the deposit type and locality. Conventional uranium processing generally involves comminution and beneficiation to concentrate uranium-bearing minerals, followed by hydrometallurgical treatment through leaching, solvent extraction or ion exchange, and precipitation to produce uranium concentrate or yellowcake ($U_3O_8$) (Lunt & El-Ansary, 2007).

In the Philippines, identified uranium occurrences are limited and are commonly associated with polymetallic and rare-earth-bearing mineral assemblages rather than conventional high-grade uranium ore systems. Earlier investigations documented uranium occurrences in the Larap–Paracale district, although these occurrences generally exhibited low uranium grades and complex mineral associations that complicate direct uranium recovery (De Guzman, 1966; Frost, 1965; Palabrica, 1978; Petrache, 1983).

One example is a Cu–Mo sulfidic and magnetite-bearing sample, which may represent a potential conventional source of uranium. However, because uranium mineralization is minor, the sample contains substantial quantities of non-uranium minerals that may interfere with downstream uranium recovery. This necessitates preconcentration of the mineralized sample prior to further processing.

Common preconcentration methods involve flotation and magnetic separation. Flotation involves using air bubbles to collect hydrophobic minerals such as sulfides with the help of collectors. The sulfides attach to the bubbles and float while the non-sulfides containing the uranium sink and can be collected for further processing. Magnetic separation, on the other hand, uses magnets to collect magnetic materials such as magnetite. In this context, the non-magnetic materials contains uranium, which can be processed for further upgrading.

This study aims to investigate the amenability of preconcentration of uranium from a Cu–Mo sulfidic and magnetite-bearing sample via magnetic separation and flotation, and to develop an integrated preconcentration process to generate potential feed material for leaching and purification toward yellowcake production.

## MATERIALS AND METHODS

**Error! Reference source not found.** summarizes the experimental flowchart of the study. The experimental procedure begins with sample preparation, including crushing, grinding, and sampling, followed by a series of characterization analyses to determine the physical, chemical, and mineralogical properties of the sample. Separate experimental tests for magnetic separation and flotation are then conducted to evaluate their respective preconcentration performances. Finally, the results from these individual tests are used to develop and evaluate an integrated preconcentration process combining magnetic separation and flotation.

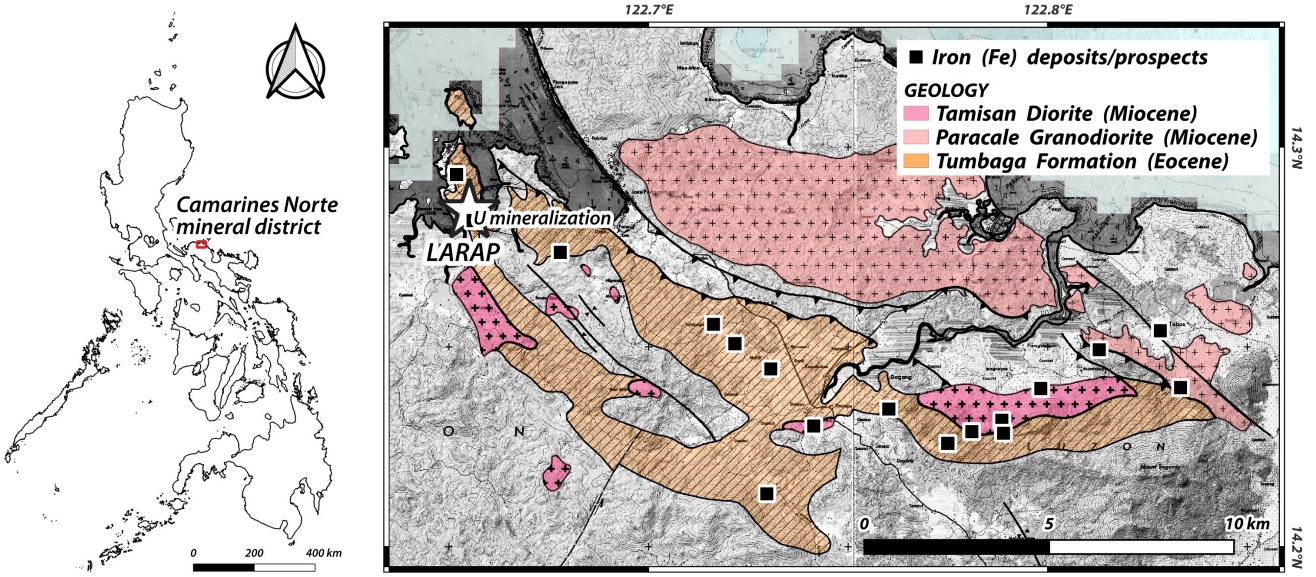


**Figure 1:** Uranium mineralization in the Camarines Norte mineral district. Location of the Cu-Mo-U mineralized sample considered in this study is marked by a star.

The sample used in this study forms part of a newly recognized surface manifestation of the uranium mineralized zones in Bessemer, Larap, the principal locale of uranium mineralization in the Camarines Norte mineral district (**Error! Reference source not found.**). This locality was originally described by Frost (1965), De Guzman (1966), and mapped at depth (~20-30m below the surface) in Tunnel 3 by Manalang (1976) and BM-PIM (1977). The sampled mineralized interval is a ~0.5 m, NE-trending NW-dipping structurally controlled uranium mineralization characterized by anomalous eU values delineated through in-situ gamma ray spectrometry surveys at 1-meter intervals. The uranium mineralized zones are within the 0.20% Cu equivalent grade shell hosted by the Eocene Tumbaga Formation (BM-PIM, 1977). Approximately 180 kilograms of the sample were collected. The Cu-Mo-U mineralized sample was primarily composed of massive orthoclase, characterized by interlocking salmon pink grains with

discernible orthogonal cleavage planes. These orthoclase grains were cut with 1-2 mm veinlets, stringers and disseminations composed of flaky and wavy biotite, soft, bluish-gray metallic molybdenite, and minute brassy metallic chalcopyrite (Figure 2a–c). Euhedral to subhedral magnetite disseminations were commonly associated with orthoclase. Under petrographic and mineragraphic analysis, 100-150 µm euhedral to subhedral uraninite grains are discerned by gray with a slight brown tinge reflection color. Uraninite occurs as disseminations and are observed to be mainly associated with interlocking mica-molybdenite-chalcopyrite-pyrite masses and veinlets, within which biotite grains are usually altered to chlorite, interlocking with orthoclase and magnetite (Figure 2d). Compared to uraninite, magnetite exhibits a more reddish tinge and crystal fractures. Molybdenite is the dominant sulfide mineral, characterized by a bright bluish-white color and kink-banded texture (Figure 2d).

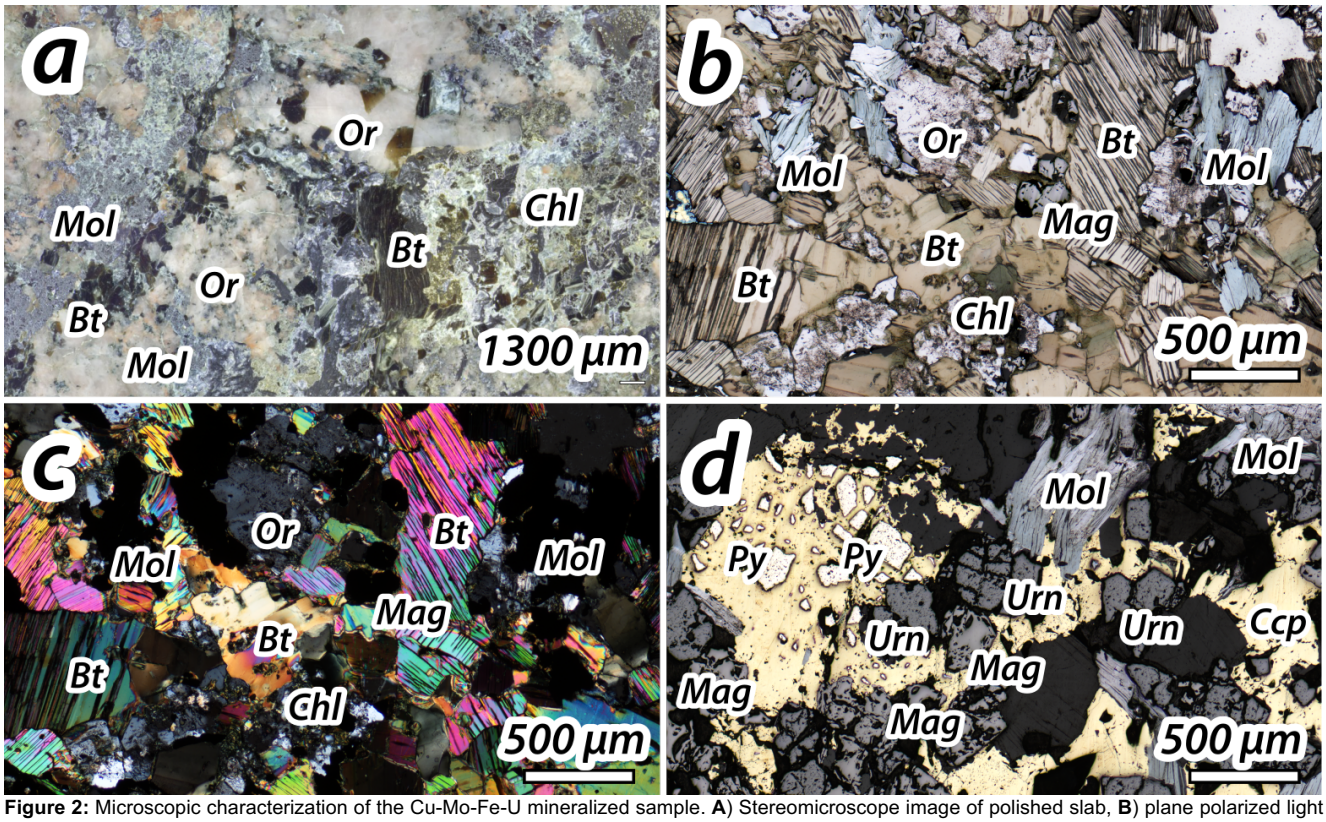


**Figure 2:** Microscopic characterization of the Cu-Mo-Fe-U mineralized sample. **A**) Stereomicroscope image of polished slab, **B**) plane polarized light photomicrograph showing silicate phases, **C**) cross polars photomicrograph, and **D**) reflected light photomicrograph showing sulfide phases. Mineral phases identified are Or-orthoclase, Bt-biotite, Chl-chlorite, Mol-molybdenite, Mag-magnetite, Py-pyrite, Ccp-chalcopyrite, and Urn-uraninite (mineral abbreviation after Warr et al., 2021).

The sample used in this study was initially subjected to primary and secondary crushing using jaw and roll crusher, respectively. The resulting crushed material was treated as a bulk sample from which representative amounts were obtained for characterization. Triple-quadrupole inductively coupled plasma mass spectrometry (ICP-QQQ) was employed to determine uranium concentrations, while inductively coupled plasma optical emission spectroscopy (ICP-OES) was employed for the analysis of all other elements. X-ray diffraction (XRD) analysis was performed to investigate the mineralogical composition of the sample and the products from the preconcentration. Particle size analysis was also performed to evaluate the distribution of uranium across the different size fractions.

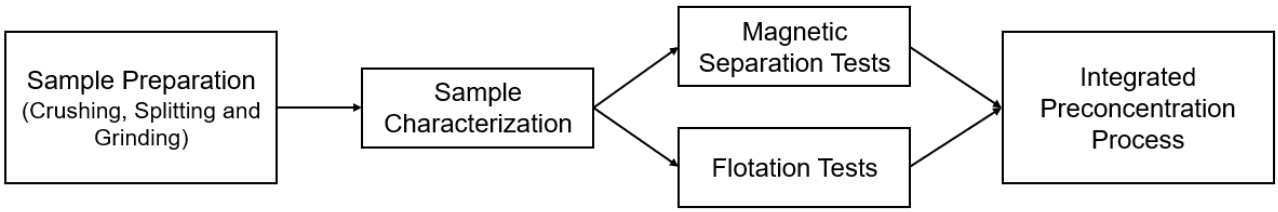


**Figure 3:** General experimental flow diagram

To evaluate the amenability of the sample to different mineral preconcentration techniques, representative samples from the bulk were obtained. Each sample underwent size reduction through wet grinding at 50% solids in a ball mill to achieve an 80% passing at 74 µm. Separate trials of magnetic separation and flotation using different xanthates and oil collectors were conducted to evaluate their influence on the recovery of the main elements — U, Cu, Mo, and Fe.

The amenability of preconcentration techniques was assessed using metal recovery (Eq. 1) which quantifies the amount of metal reporting to the product; concentration ratio, K (Eq. 2) which evaluates the extent of mass reduction; and enrichment ratio, Er (Eq. 3) which reflects the degree of impurity rejection and uranium

upgrading. A higher concentration ratio, K, indicates a greater reduction in material mass in the final product. Similarly, an enrichment ratio, Er, greater than one indicates an increase in the concentration of the target element (uranium) in the product relative to the feed.

$$\% \, Recovery = \frac{Cc}{Ff} \times 100 \qquad \textbf{Eq 1}$$

$$K = \frac{F}{C} \qquad \textbf{Eq 2}$$

$$Er = \frac{c}{f} \qquad \textbf{Eq 3}$$

where c = grade of product (ppm), f = grade of feed (ppm), C = mass of product (g) and F = mass of feed (g).

**Magnetic Separation**

Magnetic separation was performed using a laboratory-scale Davis Tube. The freshly milled sample was fed into the Davis Tube with an additional controlled water flow. The lowest setting (1 A) was used to selectively separate the magnetic minerals such as magnetite in the tube. The non-magnetic particles were washed with water and collected separately. Representative samples were obtained from both magnetic and non-magnetic fractions. These samples were subjected to analysis for elemental and mineralogical characterization.

**Flotation**

Multiple froth flotation tests were performed to evaluate the response of the material to different collectors. The collectors used for flotation experiments were composed of xanthates. Primary collectors used were sodium isobutyl xanthate (SIBX), sodium isopropyl xanthate (SIPX), and potassium amyl xanthate (PAX). Xanthates are commercially established collectors widely used in sulfide flotation, as sulfide minerals readily float in their presence. Mineral oil was also used in the study, as this is effective in recovering molybdenite. The frother used for all experiments was Dowfroth 250. The frother and collector dosage were uniform for all experimental runs at 40 µL and 40 gpt, respectively.

**Integrated Preconcentration Process**

Based on the results of the magnetic separation and flotation tests, an integrated process flow was developed. The sample was processed using the developed integrated process flow. The effectiveness of the process was measured using the metal recovery, concentration ratio, and enrichment ratio.

## RESULTS AND DISCUSSION

**Characterization**

Accurate selection of the preconcentration method requires detailed characterization of the uranium-containing material. The elemental concentration of the material is summarized in Table 1. Uranium is present at 244 ppm, which is classified as very low grade in the context of uranium ores (Dunne et al., 2019). Despite its low uranium concentration, the material contains notable amounts of copper (0.57%) and molybdenum (0.49%). This copper concentration is considered a medium grade, and with the continued global decline in average Cu ore grades (around 0.6%) and tightening copper supply (Farrell & Whitton, 2024), the industry is increasingly compelled to explore all potential sources. On the other hand, the molybdenum concentration can be classified as a high-grade suggesting that it can be a potential source for molybdenum recovery. The presence of these valuable elements justifies the need for investigation into integrated preconcentration strategies. Such an approach would not only enhance uranium recovery through effective preconcentration techniques but also enable the simultaneous extraction of copper and molybdenum, which maximizes resource utilization and improves overall extraction economics.

**Table 1:** Elemental composition of the Cu-Mo-U Mineralized Sample

| U (ppm) | Cu (%) | Mo (%) | Fe (%) |
|---|---|---|---|
| 244 | 0.57 | 0.49 | 13.5 |

To complement the elemental analysis, X-ray diffraction was employed to identify the mineral phases present. **Error! Reference source not found.** confirms the presence of uranium, copper, and molybdenum in their respective mineral phases, consistent with the elemental concentrations reported in **Error! Reference source not found.**. Specifically, uranium occurs as uraninite, copper as chalcopyrite, and molybdenum as molybdenite. The occurrence of chalcopyrite and molybdenite as sulfides — in contrast to uraninite, which is an oxide — indicates that surface-dependent concentration techniques such as flotation could be effectively applied. Furthermore, **Error! Reference source not found.** also indicates the presence of magnetite, an iron-bearing mineral, suggesting that separation through exploiting magnetic properties could also be applied.

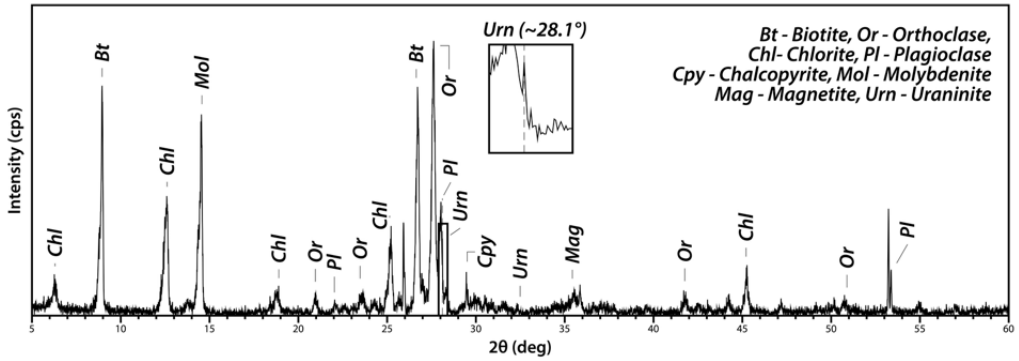


**Figure 4:** Powder XRD diffractogram of the Cu-Mo-Fe-U mineralized sample

To evaluate the distribution of uranium across the different size fractions, elemental analysis was employed on each size fraction as shown in **Error! Reference source not found.**. Uranium is predominantly distributed in the coarser size fractions. However, based on microscopic characterization in **Error! Reference source not found.**, uraninite grains are fine and associated with molybdenite, chalcopyrite, and magnetite showing that uraninite is not fully liberated at coarser sizes. This indicates that grinding is

necessary to enhance mineral liberation and improve uranium concentration efficiency. A grind size of 74 µm was therefore considered sufficient to liberate these associated minerals and facilitate effective separation.

Since physical separation processes are sensitive to particle size, fine uranium particles can significantly influence recovery. Fine particles are more prone to losses due to reduced separation efficiency, potentially through entrainment.

Understanding the elemental and mineral characteristics of the material, particularly Cu, Mo, and Fe, is essential as these factors can influence the selection of the beneficiation route. Due to the significant amounts of the gangue minerals, it is more efficient to preconcentrate uranium prior to hydrometallurgical processing. This would reduce the volume of material to be processed, which in turn would reduce reagent consumption and potentially increase efficiency and recovery.

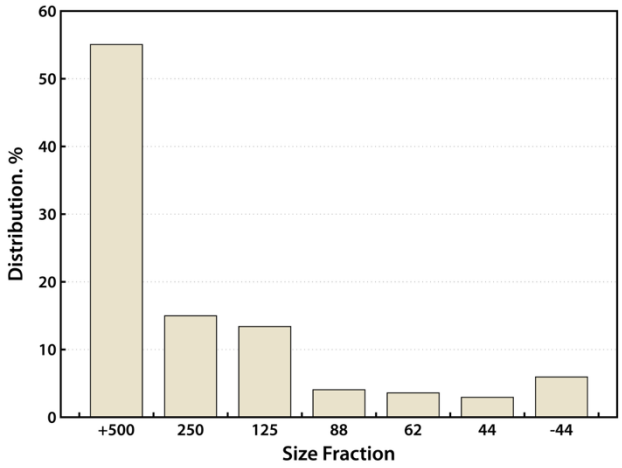


**Figure 5:** Uranium distribution in different size fraction of crushed sample

**Magnetic Separation**

Magnetic separation tests were conducted using laboratory-scale Davis Tube. The separation behavior of the target minerals was evaluated by determining the distribution of metals in the magnetic and non-magnetic fractions. Each resulting product is weighed and subjected to elemental analysis to determine the distribution of metals in the products.

The corresponding metal distribution in **Error! Reference source not found.** illustrates that most of the uranium, copper, and molybdenum reported to the non-magnetic fraction, with recoveries exceeding 90% for each element. On the other hand, approximately 50% of the iron (Fe) reported to the magnetic fraction.

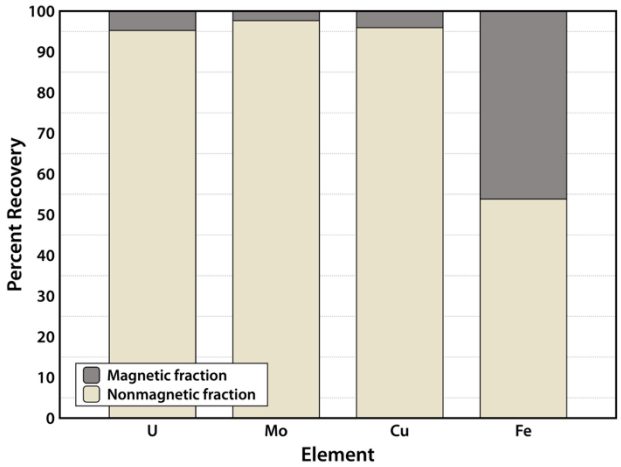


**Figure 6:** Distribution of valuable metals across the products obtained from magnetic separation tests

**Error! Reference source not found.** summarizes the elemental concentrations of the different feed and product streams, while **Error! Reference source not found.** presents the calculated concentration and enrichment ratios. The non-magnetic fraction accounted for most of the mass and contained substantially higher concentrations of uranium, molybdenum, and copper. The calculated ratios are used to evaluate the effectiveness and selectivity of the magnetic separation process. Uranium, molybdenum, and copper were substantially rejected from the magnetic stream while iron was depleted in the non-magnetic stream.

**Table 2:** Elemental concentration of U, Cu, Mo and Fe in the different streams of the circuit

| Fraction | Mass Distribution (%) | U (ppm) | Mo (ppm) | Cu (ppm) | Fe (%) |
|---|---|---|---|---|---|
| Magnetic | 13.3 | 67 | 1,702 | 2,344 | 42.5 |
| Non-magnetic | 86.7 | 206 | 10,827 | 8,464 | 7.6 |

**Table 3:** Concentration Ratio (K) and Enrichment ratios for U, Cu, Mo and Fe in the different magnetic separation product streams

| Stream | K | Enrichment Ratio | | | |
|---|---|---|---|---|---|
| | | U | Cu | Mo | Fe |
| Magnetic | 7.52 | 0.28 | 0.30 | 0.48 | 3.15 |
| Non-magnetic | 1.15 | 0.85 | 1.88 | 1.73 | 0.56 |

XRD analysis was performed to validate the occurrence of these elements in different fractions. Figure 7 provides evidence that magnetite was separated from uraninite and was recovered to the magnetic fraction, as indicated by the absence of its peaks in the non-magnetic product. Molybdenite, chalcopyrite, and uraninite were retained in the non-magnetic fraction.

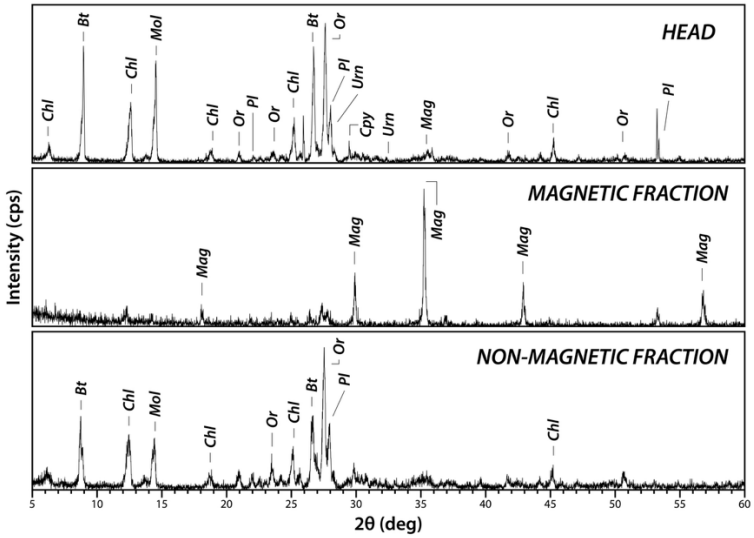


**Figure 7:** XRD analysis of head, magnetic and non-magnetic samples

The deportment of magnetite to the magnetic stream shows the effectiveness of the magnetic separation in concentrating magnetite. It should be noted that Fe is also present in other weakly magnetic minerals such as chalcopyrite and pyrite. These minerals may account for the Fe that reported to the non-magnetic fraction. Moreover, the Davis Tube test was performed using a single pass and operated at the lowest magnetic field intensity. Such conditions can reduce separation efficiency, which may account for the recovery of only approximately 50% of Fe. This presents an opportunity for further optimization through multiple passes to enhance the separation of uraninite from magnetite.

While uranium is concentrated in the non-magnetic product, magnetic separation alone is insufficient to achieve separation of U from other valuable elements, including Cu and Mo in the form of sulfides. Furthermore, gangue minerals remain in the non-magnetic stream which need to be removed through flotation. Overall, the results demonstrate that magnetic separation is an effective pre-concentration step for upgrading uranium by removing magnetic minerals.

**Flotation**

As shown in **Error! Reference source not found.**, copper and molybdenum occur as sulfides with biotite, orthoclase, and chlorite as the gangue minerals. The pronounced differences in the inherent surface properties of these minerals can be exploited to allow separation of the valuable minerals from the gangue. One of the techniques that exploits this difference is flotation. Different collectors were used to evaluate the amenability of flotation for separating sulfide minerals from the uranium-bearing phases. **Error! Reference source not found.** and **Error! Reference source not found.** illustrate the recovery of the target minerals in the concentrate and tailings under different collector conditions, respectively.

Both copper and molybdenum exhibited strong flotation response (i.e., high recovery to the concentrate) across the different reagent conditions, with consistently high recoveries obtained in the concentrate. Molybdenum reported the highest recoveries, exceeding 87% recovery in the concentrate for all collector set-ups. High molybdenum recoveries were obtained when mineral oil was used as a collector. This observation is consistent with established flotation behaviour, as oil collectors are well known to be highly effective in enhancing molybdenite flotation (Yi et al., 2021). However, despite yielding a high molybdenum recovery, the mineral oil collector resulted in the lowest copper recovery. The addition of SIPX, however, increased copper recovery.

Across all reagent conditions, uranium recovery in the concentrate remains consistently low with a maximum recovery of approximately 20%. Furthermore, the majority of uranium reported to the tailings. This behaviour confirms the limited floatability of the uraninite minerals using sulfide collectors such as xanthate. Flotation of uraninite usually requires long carbon chain collectors such as oleic acid for flotation (Agorhom et al., 2015). The presence of uranium in the concentrate can be attributed to poor liberation and entrainment (Agorhom et al., 2015). As shown in **Error! Reference source not found.**, uranium is also present in the fine particle size fraction (less than 44 µm) which has a high likelihood of being entrained in the flotation concentrate along with the sulfides. This presents an opportunity for further optimization through improved liberation or process adjustments to reduce uranium losses to the flotation concentrate.

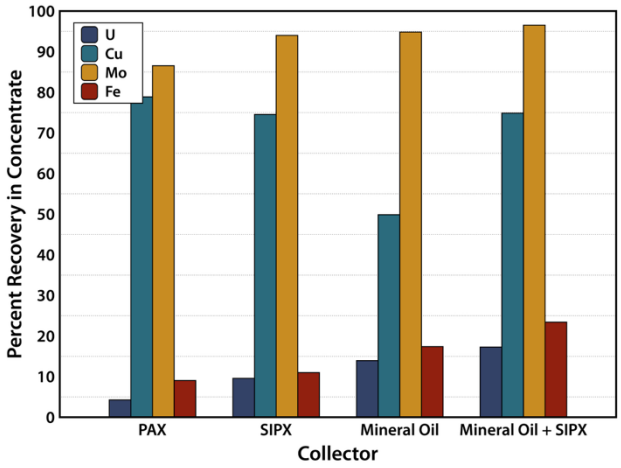


**Figure 8:** Recovery of U, Cu, Mo and Fe in the flotation concentrate using different collectors

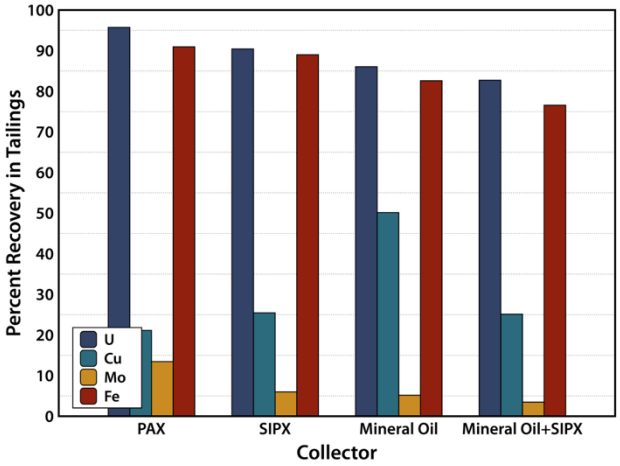


**Figure 9:** Recovery of U, Cu, Mo and Fe in the flotation tailings using different collectors

The objective of the flotation process was to upgrade uranium through the removal of chalcopyrite, molybdenite and other floatable minerals. Among the collectors tested, the use of PAX resulted in removal of 86% Mo and 79% Cu as concentrate, and U recovery of 96% as tails. The use of mineral oil together with SIPX may have resulted in the removal of high amounts of copper and molybdenum (**Error! Reference source not found.**), but this collector setting also had the least amount of uranium reporting to the tails (**Error! Reference source not found.**). This is unwanted as the aim of the study was to separate uranium from the Cu-Mo sulfide minerals. Consequently, PAX, a strong xanthate collector, was selected for the flotation step in the integrated process due to its ability to effectively float chalcopyrite and molybdenite while allowing the uraninite to remain in the tailings.

**Error! Reference source not found.** summarises the elemental concentrations of the flotation products using PAX as collector while **Error! Reference source not found.** presents the calculated concentration and enrichment ratios. The tails accounted for most of the mass and contained substantially higher concentrations of uranium. High enrichment ratios of copper and molybdenum in the concentrate indicated the efficiency of the process in enriching these elements. **Error! Reference source not found.** also confirms that sulfides have been removed as concentrate and uraninite is maintained in the flotation tailings.

**Table 4:** Elemental concentration of U, Cu, Mo and Fe in the flotation products using PAX as collector

| Stream | Mass Distribution (%) | U (ppm) | Cu (ppm) | Mo (ppm) | Fe (%) |
|---|---|---|---|---|---|
| Concentrate | 8 | 142 | 74,998 | 102,213 | 14.3 |
| Tails | 92 | 283 | 1,783 | 1,410 | 12.7 |

**Table 5:** Concentration Ratio (K) and Enrichment ratios for U, Cu, Mo and Fe in the flotation products using PAX as collector

| Stream | K | Enrichment Ratio | | | |
|---|---|---|---|---|---|
| | | U | Cu | Mo | Fe |
| Concentrate | 12.27 | 0.58 | 13.05 | 20.83 | 1.05 |
| Tails | 1.09 | 1.16 | 0.31 | 0.28 | 0.94 |

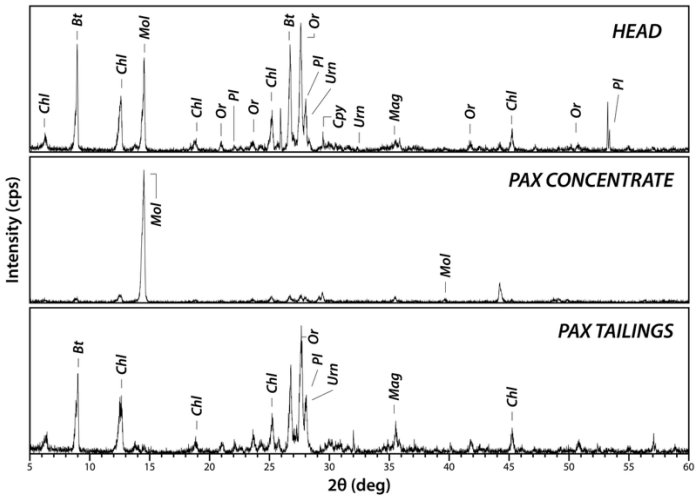


**Figure 10:** XRD analysis of flotation concentrates and tailings using PAX

**Integrated Flowsheet**

The preconcentration flowsheet for a Cu–Mo sulfidic and magnetite-bearing sample, shown in **Error! Reference source not found.**, was designed based on the results of the magnetic separation and flotation test work. The process begins with the comminution of the sample through crushing and wet grinding to achieve a $P_{80}$ of 74 µm. This is followed by flotation of the sample using PAX as collector to recover chalcopyrite and molybdenite in the concentrate and obtain uranium-enriched tailings. The resulting Cu-Mo concentrate could be further subjected to secondary flotation to separate copper and molybdenum. On the other hand, the tailings product was subjected to a magnetic separation stage. This process separated the magnetite and other magnetic minerals while concentrating uranium into the non-magnetic fraction. The inverse processing sequence (magnetic separation followed by flotation) was not evaluated due to the limited capacity of the magnetic separator and the difficulty of maintaining a consistent pulp density (% solids) required for flotation.

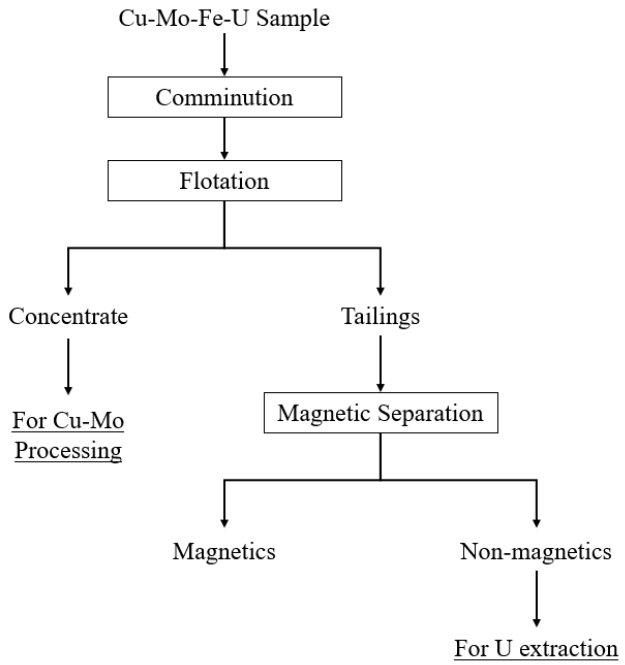


**Figure 11:** Integrated pre-concentration flowsheet using magnetic separation and flotation

Figure 12 illustrates the distribution of U, Cu, Mo and Fe across various streams. To quantitatively evaluate this elemental distribution and assess the performance of the preconcentration circuit in terms of mass reduction and grade upgrading, concentration and enrichment ratios were calculated. Table 6 summarizes the elemental concentrations of the different feed and product streams and Table 7 presents the calculated concentration and enrichment ratios.

Copper and molybdenum predominantly reported to the flotation concentrate, which accounts for most of their total distribution. The enrichment ratios of Cu and Mo in the concentrate were significantly greater than 1, indicating that Cu and Mo were effectively enriched in the flotation concentrate and separated from the uranium-enriched flotation tailings. Iron was largely concentrated in the magnetic fraction, which indicates the presence of magnetite.

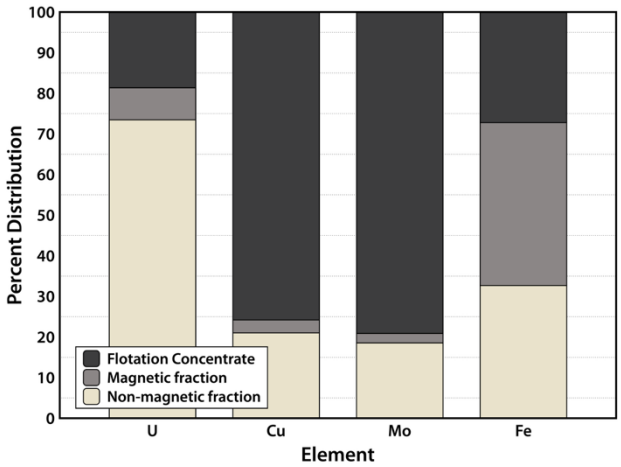


**Figure 12:** Overall distribution of U, Cu, Mo and Fe across the different overall process streams

The majority of uranium reported to the non-magnetic stream; however, a substantial proportion (approximately 20%) also reported to the flotation concentrate with the remainder to the magnetic fraction. **Error! Reference source not found.** shows that the uranium grade increases significantly in the final non-magnetic stream, increasing from 244 ppm in the feed to 305 ppm. Additionally, the different calculated ratios in **Error! Reference source not found.** further validate that uranium is preferentially upgraded in the non-magnetic stream, achieving a uranium enrichment ratio of 1.25. The relatively low concentration ratio is expected since no additional process was conducted to remove the other gangue minerals in the non-magnetic fraction. The increase in uranium grade and the removal of other minerals indicate that the integrated process effectively reduces material volume while enhancing uranium concentration by approximately 25% of the feed grade.

**Table 6:** Elemental concentration of U, Cu, Mo and Fe in the different streams of the circuit

| Stream | Mass Distribution (%) | U (ppm) | Cu (ppm) | Mo (ppm) | Fe (%) |
|---|---|---|---|---|---|
| Feed | - | 244 | 5,745 | 4,905 | 13.50 |
| Concentrate | 27 | 176 | 17,162 | 15,200 | 14.4 |
| Magnetic | 13 | 149 | 1,441 | 902 | 42.50 |
| Non-magnetic (Final) | 60 | 305 | 2,092 | 1,566 | 7.60 |

**Table 7:** Concentration Ratio (K) and Enrichment ratios for U, Cu, Mo and Fe in the different product streams

| Stream | K | Enrichment Ratio | | | |
|---|---|---|---|---|---|
| | | U | Cu | Mo | Fe |
| Concentrate | 3.8 | 0.95 | 2.99 | 3.10 | 1.07 |
| Magnetic | 7.6 | 0.80 | 0.25 | 0.18 | 3.15 |
| Non-magnetic | 1.7 | 1.25 | 0.36 | 0.32 | 0.56 |

In addition, as shown in the microscopic characterization in **Error! Reference source not found.** each of the grains is well liberated from its associated minerals. The uraninite grain maintains its subhedral profile at ~50 µm in diameter, free from the chalcopyrite-molybdenite-pyrite matrix it usually associates with.

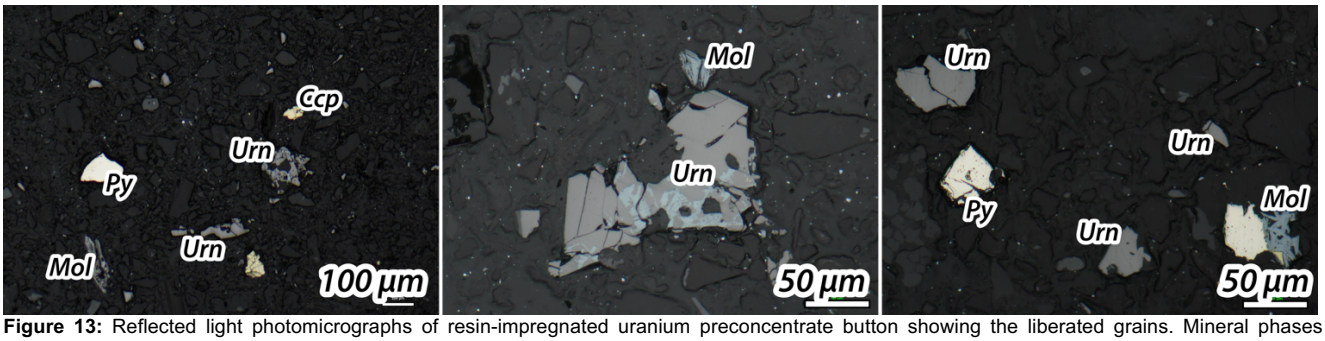


**Figure 13:** Reflected light photomicrographs of resin-impregnated uranium preconcentrate button showing the liberated grains. Mineral phases identified are Mol-molybdenite, Mag-magnetite, Py-pyrite, Ccp-chalcopyrite, and Urn-uraninite.

Overall, the integrated preconcentration process achieved a concentration ratio of 1.7 and an enrichment ratio of 1.25, increasing the uranium grade to 305 ppm at 73% U recovery. Despite the improved uranium upgrade, a significant proportion of uranium (approximately 20-27%) reported to the flotation concentrate and magnetic streams. The incorporation of cleaner stages in both flotation and magnetic separation presents a potential opportunity to reduce uranium losses and enhance overall uranium recovery.

These results demonstrate that the proposed process effectively reduced material volume while increasing uranium grade, producing a suitable feed for further leaching and purification toward yellowcake production. Moreover, the preconcentration process also demonstrates capability in recovering copper (chalcopyrite), molybdenum (molybdenite) and magnetite.

## CONCLUSION

The integrated process for preconcentrating uranium from a Cu–Mo sulfidic and magnetite-bearing sample effectively preconcentrated uranium in the non-magnetic fraction, while separating copper and molybdenum in the flotation concentrate and iron in the magnetic separation concentrate. The process yielded a concentration ratio of 1.7, and a uranium enrichment ratio of 1.25 at 73% U recovery. This non-magnetic product presents a suitable feed for further processing toward yellowcake production. These findings suggest that a combined approach of flotation-magnetic separation offers a promising preconcentration strategy for upgrading uranium from Cu–Mo sulfidic and magnetite-bearing samples.

## ACKNOWLEDGMENTS

This work is funded by the Department of Science and Technology - Grants-in-Aid (DOST-GIA) Program through the NuCycle Program – NuMER project. The authors would like to extend their gratitude to the University of the Philippines Diliman Department of Mining, Metallurgical, and Materials Engineering (UPD DMMME), and the Department of Science and Technology - Philippine Nuclear Research Institute (DOST-PNRI) for the support of this research work.

## CONFLICT OF INTEREST

The authors declare that there is no conflict of interest.

## CONTRIBUTIONS OF INDIVIDUAL AUTHORS

- **Terrence Louis A. Rosal** - Conceptualization, sampling, experimental design, flotation and magnetic separation experiments, data analysis, and preparation of the original manuscript
- **John Rossmon M. Resuello** - Assisted in experimental design, data analysis, integrated flotation and magnetic separation experiments, and critical revision of the manuscript
- **Leslie Marie B. Red** - Conceptualization, sampling, experimental design, flotation and magnetic separation experiments, data analysis, and critical revision of the manuscript
- **Lawrence Glen F. Sabaria** – Sampling, petrographic analysis, XRD & WD-XRF analyses, assisted in data interpretation, flotation and magnetic separation experiments.
- **Pearlyn C. Manalo** –Sample preparation, XRD & WD-XRF analyses.
- **Americus dC. Perez** - Conceptualization, sampling, experimental design, flotation and magnetic separation experiments, data visualization and analysis, and contributed to manuscript review and editing
- **Angel T. Bautista VII** – Conceptualization, provided supervision, laboratory resources, funding acquisition, and contributed to manuscript review and editing
- **Djoan Kate T. Tungpalan** - Conceptualization, sampling, experimental design, flotation and magnetic separation experiments, data analysis, provided supervision, laboratory resources, funding acquisition, and contributed to manuscript review and editing

## REFERENCES

Agorhom, E. A., Lem, J. P., Skinner, W., & Zanin, M. (2015). Challenges and opportunities in the recovery/rejection of trace elements in copper flotation-a review. *Minerals Engineering*, *78*, 45-57. https://doi.org/10.1016/j.mineng.2015.04.008

Andal, A. G., PraveenKumar, S., Andal, E. G., Qasim, M. A., & Velkin, V. I. (2022). Perspectives on the Barriers to Nuclear Power Generation in the Philippines: Prospects for Directions in Energy Research in the Global South. *Inventions (Basel)*, *7*(3), 53. https://doi.org/10.3390/inventions7030053

BM-PIM. (1977). *PIM-Uranium Project*.

Cuney, M. (2010). Evolution of uranium fractionation processes through time; driving the secular variation of uranium deposit types. *Economic geology and the bulletin of the Society of Economic Geologists*, *105*(3), 553-569. https://doi.org/10.2113/gsecongeo.105.3.553

De Guzman, R. A., Estupigan, P. S., & Luis, R. M. (1966). *Uranium Mineralization in the Paracale District Camarines Norte*

Dixon, L., Yeganyan, R., Tan, N., Cannone, C., Howells, M., Foster, V., & Plazas-Niño, F. (2025). The Philippines' Energy Transition: Assessing Emerging Technology Options Using OSeMOSYS (Open-Source Energy Modelling System). *Climate (Basel)*, *13*(1), 14. https://doi.org/10.3390/cli13010014

Dunne, R. C., Kawatra, S. K., & Young, C. A. (2019). *SME Mineral Processing & Extractive Metallurgy Handbook* (1 ed.). Society for Mining, Metallurgy, and Exploration (SME).

Farrell, S., & Whitton, L. (2024). BHP Insights: how copper will shape our future. Retrieved March 14, 2026, from https://www.bhp.com/news/bhp-insights/2024/09/how-copper-will-shape-our-future.

Frost, J. E. (1965). *Controls of ore deposition for the Larap mineral deposits, Camarines Norte, Philippines* Stanford University].

Gulagi, A., Alcanzare, M., Bogdanov, D., Esparcia, E., Ocon, J., & Breyer, C. (2021). Transition pathway towards 100% renewable energy across the sectors of power, heat, transport, and desalination for the Philippines. *Renewable & sustainable energy reviews*, *144*, 110934. https://doi.org/10.1016/j.rser.2021.110934

Lunt, D., Boshoff, P., M, B., & El-Ansary, Z. (2007). Uranium extraction: the key process drivers. *Journal of the South African Institute of Mining and Metallurgy*, *107*(7), 419-426.

Manalang, E., Baguilat, C., & Rovillos, P. (1976). *Radiometric Survey and Preliminary Geologic Estimate of Uranium Tonnage at Tunnel 3 in Bessemer Rescue Area of Philippine Iron Mines, Larap, Jose Panganiban, Camarines Norte*

Mondal, M. A. H., Rosegrant, M., Ringler, C., Pradesha, A., & Valmonte-Santos, R. (2018). The Philippines energy future and low-carbon development strategies. *Energy (Oxford)*, *147*, 142-154. https://doi.org/10.1016/j.energy.2018.01.039

NEA. (2025). *Uranium 2024: Resources, Production and Demand*.

Palabrica, O. T., Alonso, C.V., Cortes, A.B., Santos, G. Jr. (1978). Preliminary Laboratory Practices on the Recovery of Uranium from Larap Ores. *Philippine Metals*, 20-28.

Petrache, C. A., Marcelo, E.A., Macadangdang, J.K., Daud, A.H.H., Bahari, K. (1983). Preliminary tests on the recovery of uranium from Larap drill cores. In P. A. E. Commission (Ed.).

Warr LN. IMA–CNMNC approved mineral symbols. *Mineralogical Magazine*. 2021;85(3):291-320. doi:10.1180/mgm.2021.43

Yi, G., Macha, E., Van Dyke, J., Ed Macha, R., McKay, T., & Free, M. L. (2021). Recent progress on research of molybdenite flotation: A review. *Advances in Colloid and Interface Science*, *295*, 102466. https://doi.org/10.1016/j.cis.2021.102466